MONITORING CRACKED SHAFT BY USING ACTIVE ELECTRO-MAGNETIC ACTUATOR - NUMERICAL SIMULATION

Tobias Souza Morais, tobiassouza@yahoo.com.br
Valder Steffen Jr, vsteffen@ufu.com.br
Federal University of Uberlandia, School of Mechanical Engineering, Campus Santa Monica, 38400-902 Uberlandia – MG - Brazil
Jarir Mahfoud, jarir.mahfoud@insa-lyon.fr
Johan Der Hagopian, johan.derhagopian@insa-lyon.fr
Laboratoire des Mécanique des Contacts et des Structure – LaMCoS, UMR CNRS 5259, Institut National de Sciences Appliquées de Lyon, 69621 Villeurbanne Cedex, France

Abstract. *The paper is a numerical study aiming at assessing the possibility of monitoring the dynamic behavior of a rotating machine with a cracked shaft by using Electro-Magnetic Actuator (EMA). The system studied is composed of a horizontal flexible shaft with two rigid discs. The shaft is supported by bearings located at its ends: A roller bearing at one end and two ball bearings at the other end. A EMA located in the middle of the rotor constitute the smart active bearing and provide the active control. The opening and the closure (breathing) of the crack is determined by the stress field over its cross section, caused by the dynamic bending moment. The hypothesis of heavy rotor, for which the dynamic behavior of the crack (opening and closure) is only function of the rotor angular position, is not considered in the present contribution. Here, the system is highly nonlinear due to the fact that the crack parameters must be determined for each time step. The model developed take into account the behavior of the crack and the influence of the EMA. The results obtained demonstrate on the possibility of using EMA in order to keep the crack closed along the rotation of the rotor, thus forming a self healing scheme for the cracked rotor.*

Keywords*: Rotordynamics; Electro-Magnetic Actuator; Cracked Rotors*

1. INTRODUCTION

Great catastrophic failures in rotating machines are commonly due to the propagation of cracks as caused by fatigue. Significant research effort is being developed in the last twenty years aiming at detecting cracks. More recently, in the context of structural health monitoring and maintenance, the safely operation of cracked shafts is desired to continue for the longest possible time, before replacement. In industrial applications it is known that cracked shafts can be kept under operation for many years, if correctly monitored and operated, before being replaced. As the fatigue process in rotating shafts is characterized by the crack opening and closing during rotation, this paper proposes a way to keep the system working in attempt to slow down the progress of the fatigue mechanism. This is achieved by using an Electro-Magnetic Actuator (EMA), which controls the dynamics of the system so that the total opening of the crack is avoided. In 2003, Changsheng Zhu et al. described a number of difficulties associated to crack identification in shafts supported by magnetic bearings. Quoting these authors, "it is impossible to use the traditional method with the 2X and 3X revolution super-harmonic frequency components in the super-critical speed region to detect the crack.". In 2006, Mani et.al. reported to have accomplished the active health monitoring of rotordynamic systems in the presence of cracked shafts performing the breathing phenomenon. In both papers, the crack model used does not consider the breathing behavior of the crack as a function of dynamical behavior of the structure, but only as a function of the rotor angular position. Thus, the active magnetic bearing does not influence the crack dynamics. In this paper, the crack model depends on the dynamic moment which acts in the ends of the cracked element. The active magnetic actuator is used to compose a self-healing system so that the rotor can continue its operation since the increase of the fatigue crack is avoided. Evidently, the authors are aware that the introduction of an Electro-Magnetic Actuator intended to crack control in a system that was not designed accordingly is not simple and can be very costly. However, the present contribution is focused on the modeling and simulation of rotating systems with two non-linear factors: a crack that causes shaft stiffness variation as a function of the structure dynamics and the EMA that is designed to apply forces that are inversely proportional to the square of the gap value between the stator and the rotor so that the fatigue life of the cracked rotor is increased. This leads to a new possible use of active magnetic bearings.

2. METHODOLOGY DESCRIPTION

A differential equation that expresses the dynamic behavior of a flexible cracked rotor with EMA can be written as follows:

$$[M]\{\ddot{x}(t)\} + \left[C_b + \dot{\emptyset}C_g\right]\{\dot{x}(t)\} + \left[K(t) + \ddot{\emptyset}K_g\right]\{x(t)\} = F_u(t) + F_{EMA}(t) \quad (1)$$

where: $\{x(t)\}$ is the generalized displacement vector; $[M]$, $[C_b]$, $\left[C_g\right]$ and $\left[K_g\right]$ are the well known matrices of inertia, bearing viscous damping, gyroscopic effect with respect to the rotation velocity and gyroscopic effect in relation to the rotation acceleration, respectively (Lalanne, 1998). $\dot{\emptyset}$ is the angular velocity. $[K(t)]$ is the stiffness matrix with

the cracked element, and $F_u(t)$ and $F_{EMA}(t)$ are forces due to the unbalance and the Electro-Magnetic Actuator (EMA), respectively.

The system studied is presented in the Fig. (1). It is composed of a horizontal flexible shaft of 0.0402 m of diameter and two discs represented by D_1 and D_2. The shaft is supported by symmetric bearings at its ends: two ball bearings at the left hand end (2.10^8 N/m stiffness and 800N.s/m damping) and a roller bearing at the right hand end (1.10^6 N/m and 800N.s/m). The EMB is represented by B_2. A finite element model (Fig. (2)) was used to carry out the numerical simulations of the system. For this aim, the model contains the following elements: rigid discs with only kinetic energy contribution, flexible shaft with kinetic and strain energy as represented by Timoshenko beam elements with two nodes per element and 4 d.o.f per node. The dynamics of the FEM model was studied by using a MATLAB code and the unbalance response was compared with the software ROTORINSA for validation purposes. The simulation was performed by using the MATLAB/SIMULINK package. The SIMPLE optimization toolbox was used to identify the electric current of the EMA as will be described in a following section. Only the displacement response generated by using the first eight modes at the EMA position was considered for all analyses performed in the present contribution.

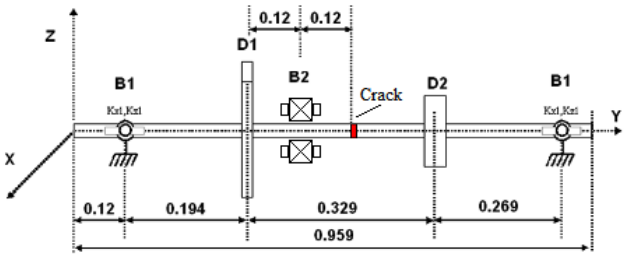

Figure 1. Rotor System Studied

The stiffness matrix of the cracked element and the EMA are described in the following. Both the crack and the EMA positions can be seen in the Figs. (1) and (2).

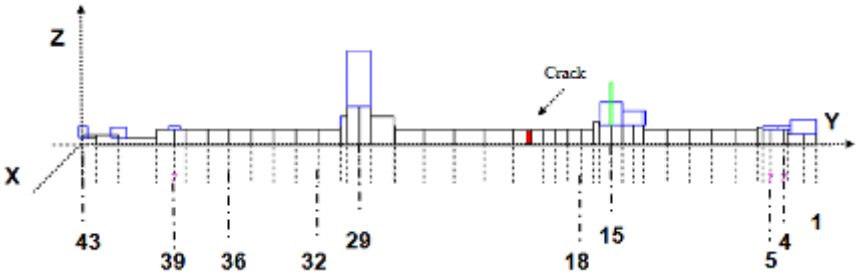

Figure 2. Rotor Finite Element Model

3. MODELLING OF THE BREATHING MECHANISM

The breathing mechanism is a result of the stress and strain distribution around the cracked area, which is due to static loads (like the weight), the bearing reaction forces, and the dynamical loads (such as the unbalance and the vibration induced inertia force distribution). When the static loads overcome the dynamical ones, the breathing is governed by the angular position of the shaft with respect to the stationary load direction, and the crack opens and closes again completely once each revolution. The transition from closed crack (full stiffness) to the open crack (weak stiffness) has been generally considered abrupt (Gasch, 1993) or represented by a given cosine function, but can be calculated step by step through an iterative procedure as considered here. The opening and the closure (breathing) of the crack is determined by the stress field over its cross section as caused by the dynamic bending moments. The hypothesis of heavy rotor, for which the dynamic behavior of the crack (opening and closure) is only a function of the rotor angular position, is discarded in the present contribution. Here, the system is nonlinear and consequently the crack parameters must be determined for each time step. Breathing behavior calculation is summarized in the flowchart shown in Fig. (3). The identification process starts with the estimation of the crack parameters and the modeling of the structure through the finite element method. It is known that the crack influences only the parameters of stiffness. Consequently, the other parameters do not change in the presence of a crack. For determining the stiffness matrix of the cracked element, $K_c(t)$, it is necessary to calculate first the second moments of inertia of the cross section where the crack is located. For this aim, the cross section is meshed as shown in Fig. (4). Then the geometric center and the moments with respect to this point are obtained. The opening and closure of the crack are given as a function of the stress field resulting from the dynamic efforts and weight of the structure (Paolo Pennacchi, 2005).

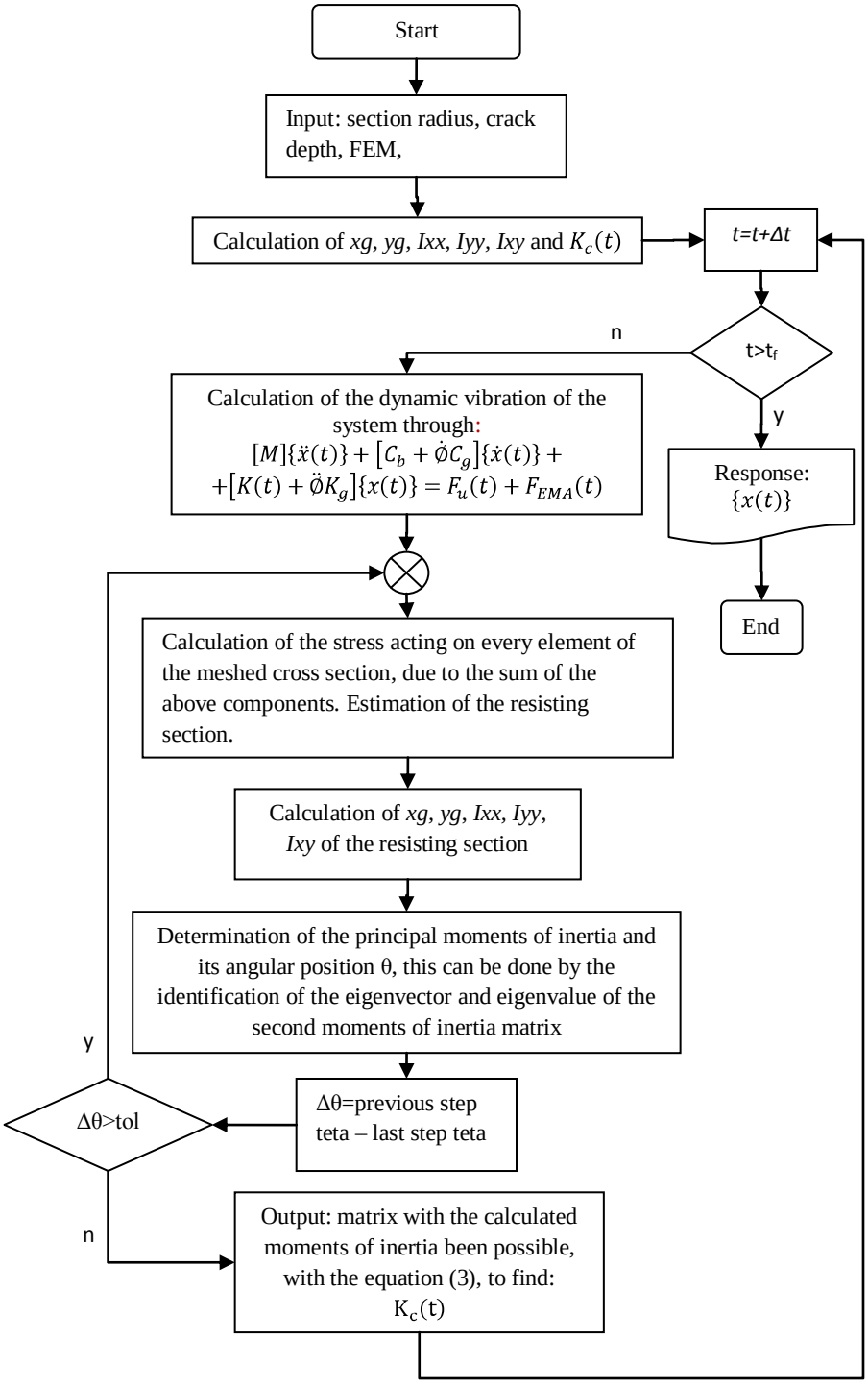

Figure 3. Flowchart for the iterative calculation of the breathing mechanism with the EMA

The tension should be calculated for each element of the meshed cross section, Fig. (4). If the stress field along the crack is positive, it means that the region is under traction, i.e., the crack is opened and does not contribute to the calculation of the moment of inertia. Consequently, a reduction is observed in the values of the elements of the stiffness matrix. On the other hand, if the field along the crack is negative, the region is under compression, i.e., the crack is considered closed thus contributing to the moment of inertia of the cross section and to the corresponding stiffness elements in the matrix.

Due to the cross section asymmetry, the stress given by:

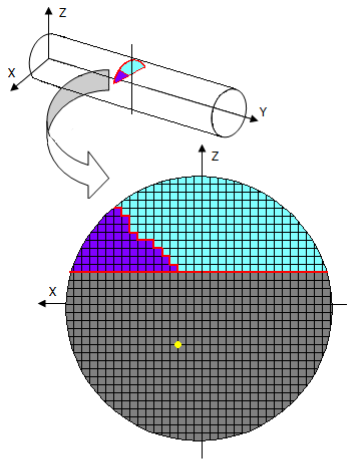

Figure 4. Cross section of the cracked element

$$\sigma = \frac{M_z I_{xx} + M_x I_{xz}}{I_{xx} I_{zz} - I_{xz}^2} x - \frac{M_x I_{zz} + M_z I_{xz}}{I_{xx} I_{zz} - I_{xz}^2} z \quad (2)$$

The dynamic moments M_x and M_z are given from the strength of materials theory: $\frac{\partial \theta_x}{\partial y} = \frac{M_x}{EI}$ and $\frac{\partial \theta_z}{\partial y} = \frac{M_z}{EI}$ where θ_x and θ_z are the rotations with respect to the axes x and z, respectively. In practice, $\partial\theta_x = \theta_x^{i+1} - \theta_x^i$ is considered, where i is the node at the end of cracked element and $\partial y = L_c$, where L_c is the length of this element, as illustrated in the Fig. (5).

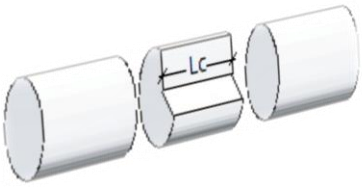

Figure 5.Equivalent cracked beam element: its configuration changes with its angular position

3.1 Equivalent beam stiffness matrix

Once the breathing mechanism and the second moments of area have been defined, as previously described, the stiffness matrix of an equivalent cracked beam element of suitable length L_c can be calculated, assuming a Timoshenko's beam with constant cross section and second moments of area along L_c, as shown in Fig. (5). The neighboring beam elements are simply circular cross section beams.

In the Fig. (6) the fitting between the simplified Flex model and the 3D model to determine an optimal length value of the cracked element (Bachschmid et.al. 2003) can be observed.

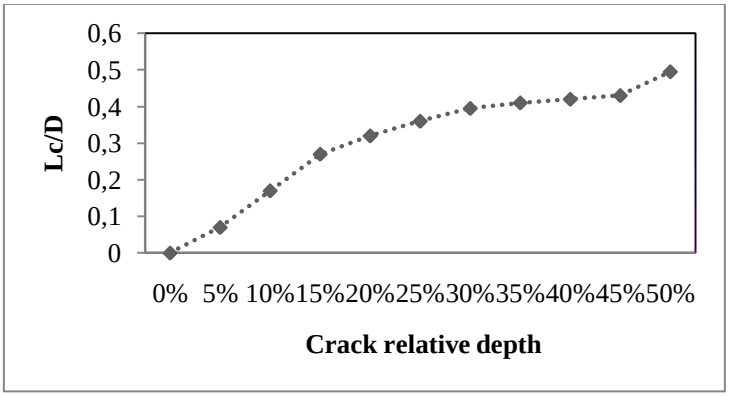

Figure 6. Relationship between the crack relative depth p, the diameter D and the length L_c of "equivalent" beam

The stiffness matrix (square, 8×8 symmetrical matrix) is represented by equation (3). More details regarding the identification of this matrix can be found in Bachschmid et.al. 2003.

$$K_c(t) = \begin{bmatrix} b & p & -q & -d & -b & -p & -q & -d \\ p & a & c & q & -p & -a & c & q \\ -q & c & e & r & q & -c & f & s \\ -d & q & r & h & d & -q & s & g \\ -b & -p & q & d & b & p & q & d \\ -p & -a & -c & -q & p & a & -c & -q \\ -q & c & f & s & q & -c & e & r \\ -d & q & s & g & d & -q & r & h \end{bmatrix} \begin{Bmatrix} x_i \\ z_i \\ \theta_{x\,i} \\ \theta_{z\,i} \\ x_{i+1} \\ z_{i+1} \\ \theta_{x\,i+1} \\ \theta_{z\,i+1} \end{Bmatrix} \quad (3)$$

where the coefficients above are defined as:

$$a = \frac{12\, I_{yy} E}{(1+\phi) L_c^3}, b = \frac{12 I_{xx} E}{(1+\phi) L_c^3}, c = \frac{6 I_{yy} E}{(1+\phi) L_c^2}, d = \frac{(4+\phi) I_{yy} E}{(1+\phi) L_c}, f = \frac{(2-\phi) I_{yy} E}{(1+\phi) L_c}, g = \frac{(2-\phi) I_{xx} E}{(1+\phi) L_c}, h = \frac{(4+\phi) I_{xx} E}{(1+\phi) L_c}, p = \frac{12\, I_{xy} E}{(1+\phi) L_c^3}, q = \frac{6 I_{xy} E}{(1+\phi) L_c^2}, r = \frac{(4+\phi) I_{xy} E}{(1+\phi) L_c}, s = \frac{(2-\phi) I_{xy} E}{(1+\phi) L_c}, \phi = \frac{12 EI}{GSL_c^2}$$

.

The parameter ϕ accounts for the shear effects, E and G are respectively the Young's modulus and the shear modulus, S is the cross section area, and I are the second moments of area.

4. THE ELECTRO-MAGNETIC ACTUATOR

The Electro-Magnetic Actuator (EMA) considered in this paper consists of 4 electromagnetic coils; each one applies an attraction force (Damien, 2003) given by Eq. (4). In the Fig. (7) we can see the system configuration.

$$F_{em} = \frac{N^2.I^2.\mu_0.a.f}{2\left(e + \frac{b+c+d-2a}{\mu_r}\right)^2} \tag{4}$$

The values of the coil parameters are given in table (1).
Table 1. Parameters of the coil.

μ_0 (H/m)	1.2566E-06
μ_r (H/m)	700
N (Spires)	278
a (mm)	21
b (mm)	84
c (mm)	63
d (mm)	21
f (mm)	42
e^* (mm)	1.5

The forces applied by the electromagnetic actuators are written as a function of the inverse of the square gap value and it varies along the vibration of the structure, i.e., they depend on the rotor displacement at the bearing position, resulting a nonlinear actuator.

The currents used to feed the coils were designed so that they exhibit two terms, namely a constant current in each coil that is added to a varying current depending on the crack angular position, aiming at producing an attraction force that is sufficiently large to avoid the total opening and small enough to not increasing significantly the displacements of the structure, which would lead the system collapse. The varying currents follow a sinusoidal law, which begins at the time when the point P (crack placement point) passes to the opposite side of the coil, reaches a maximum value when P is at the most distant position with respect to the coil and is zero when it passes to the side of the coil, as shown in the Fig. (7) where a constant current of 0.3 A was used in each coil. For the case in which the rotor performs an inverse whirl movement the configuration of these currents is such that they keep the crack open, i.e., their feature is precisely the opposite of the one illustrated in the Fig. (7).

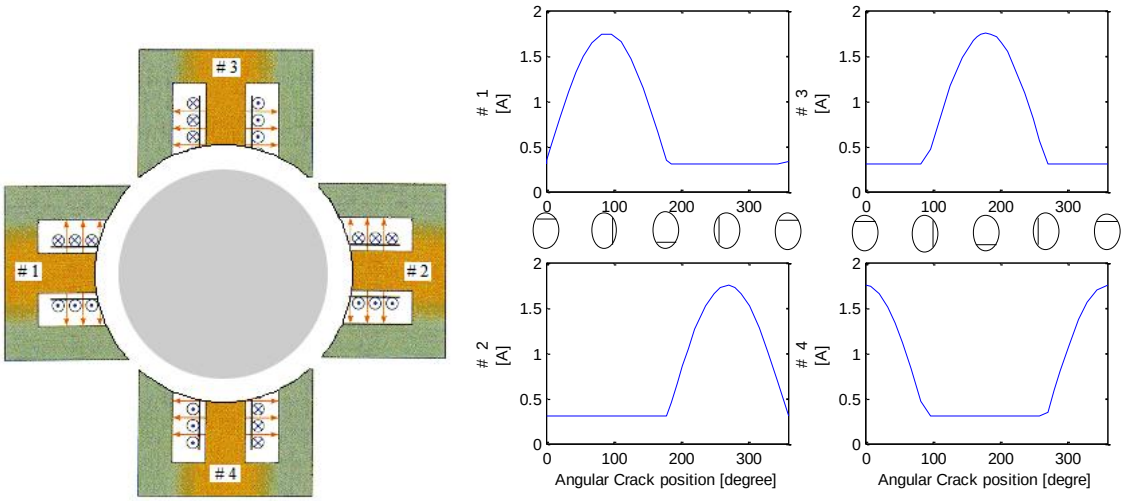

Figure 7. Electric current in each coil as a function of the angular rotor position

4.1 Identification of the coil current

The procedure to minimize the crack opening can increase the vibration level of the rotor, which leads to undesired side effects. Consequently, the goal of the proposed technique at this point is to determine a current combination that is capable of minimizing the crack opening and, at the same time, does not induce large vibrations to the system. For this aim, a pseudo-random optimization method, the particle swarm optimization (PSO), was used. 120 individuals were considered and 80 iterations were performed. The multi-objective function takes into account *i)* the reduction of the crack opening, Eq. (5), and *ii)* the minimization of the system vibration, Eqs. (6) and (7), as measured in the x and z directions, respectively, at the position of the EMA. The design variables considered are the following: four constant currents and four variable currents for the coils, thus totalizing eight variables. The currents range from 0 to 5 A. Figure

(8) shows the variation of the unbalance response for different values of the electric current in the case of constant currents applied to the coils. It can be seen that the vibration amplitude decreases as the current intensity increases, for determined speed rotation ranges. This behavior justifies the methodology presented. Another important point for using CC is related to the rotor mounted horizontally in which the weight influences the dynamics of the crack significantly. Finally, it is expected that the optimization method is able to find zero current intensity depending on the given rotation speed; also different current intensities are supposed to be found, for the rotor either in the horizontal or vertical arrangements.

$$F_1 = \sum_{j=1}^{np}\left(S_j - Ar_j\right)^2 \Big/ \sum_{j=1}^{np}\left(S_j\right)^2 \tag{5}$$

$$F_2 = \sum_{j=1}^{np}\left(x_j\right)^2 \tag{6}$$

$$F_3 = \sum_{j=1}^{np}\left(z_j\right)^2 \tag{7}$$

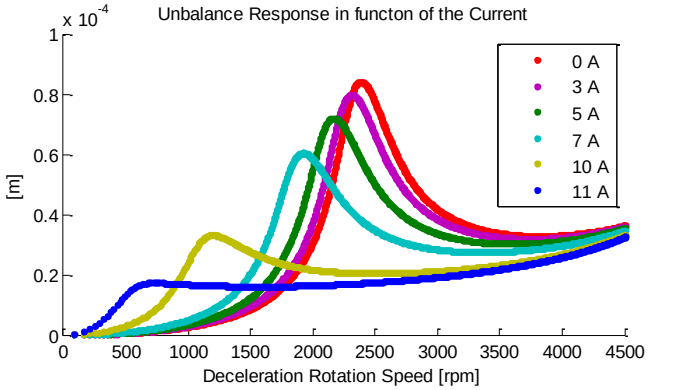

Figure 8. Unbalance Response for a non cracked rotor as a function of the current

5. RESULTS AND DISCUSSION

Two case studies will be addressed by using the same system configuration. First, a flexible rotor was mounted in the vertical position so that the weight does not influence the crack dynamics; second, the same rotor was mounted horizontally so that the weight is an important factor in the dynamics of the crack. For simulation purposes, the crack depth used was equal to the axis radius and the length of the cracked element was determined according to the Fig. (6).

5.1. Vertical Rotor

The system was simulated considering the gravity force as being equal to zero, thus the crack breathing is given as a function of the structure dynamic efforts, only. An unbalance of 80 g.cm and phase 0 was applied to the first disc at a rotation speed of 1500 rpm. The results found by using the optimization method are given as follows: for the continuous currents – no driving current for the 4 coils (null currents); for the varying currents - the current amplitudes are 1.801 A for the coil #1, 1.799 A for the coil #2 and 0.333A for the coils #3 and #4. As seen in the Fig. (8) the continuous currents in the coils would make the vibration level to increase for the rotation speed considered. This behavior validates the result given above for these currents (they are all zero). These results were found for a sampling time of 1 second so that the EMA was turned off for t=0.7 sec.

In the Fig. (9) the responses measured at the EMA position are shown along the in x and y directions, respectively. Figures (10) and (11) show the variations of the cross section area and the second moments of area of the element cross section as a function of time, respectively. The crack is kept relatively closed. In the Fig. (12) the currents applied to the coils are presented and in the Fig. (13) the corresponding required forces are shown. For the configuration of the currents considered in the present design, as presented in the Fig. (7), the electromagnetic force in the x direction is considerably higher than the one along the z direction.

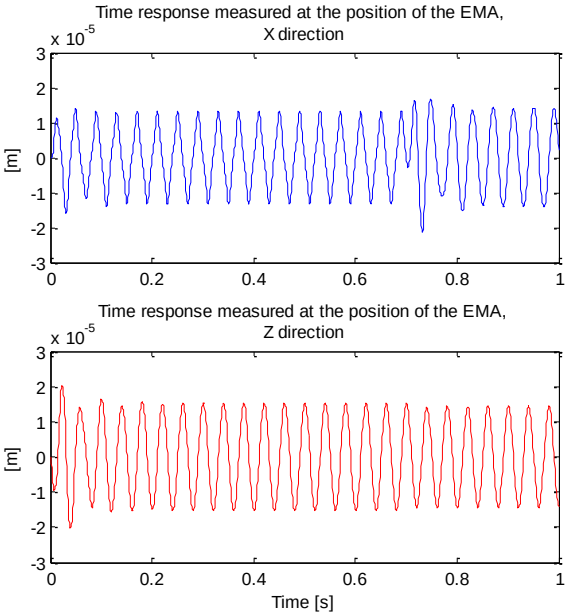

Figure 9. Response of the system

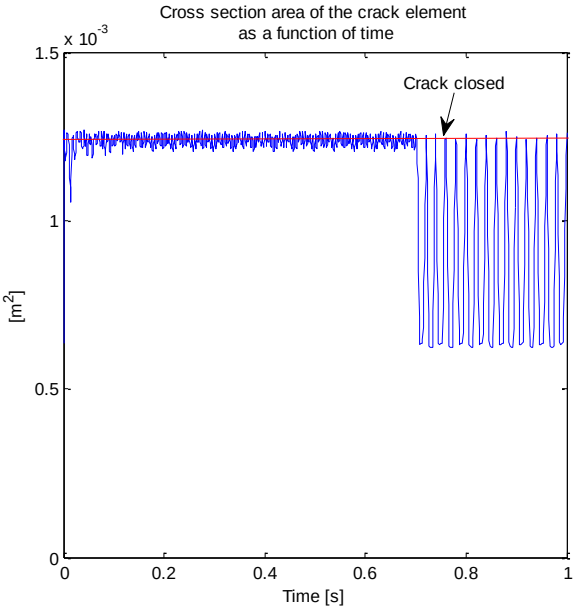

Figure 10. Cross Section of the cracked element

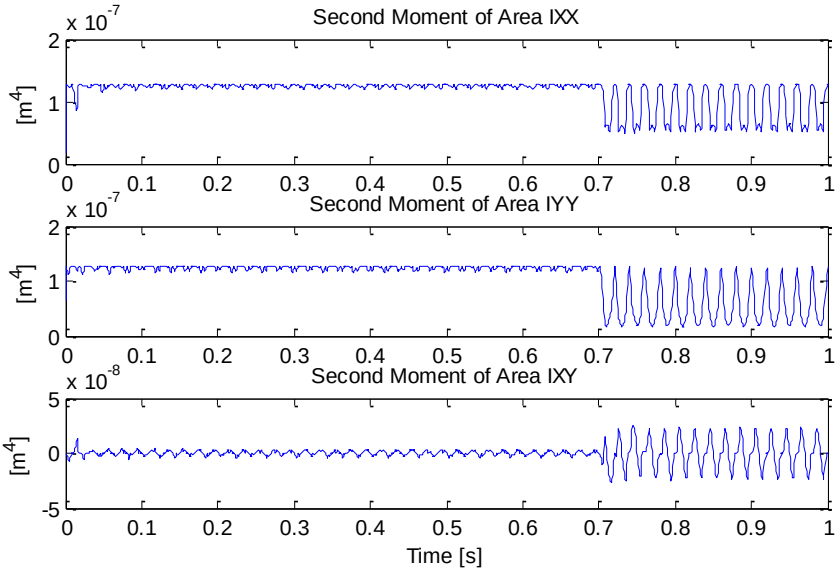

Figure 11 Second Moments of Area

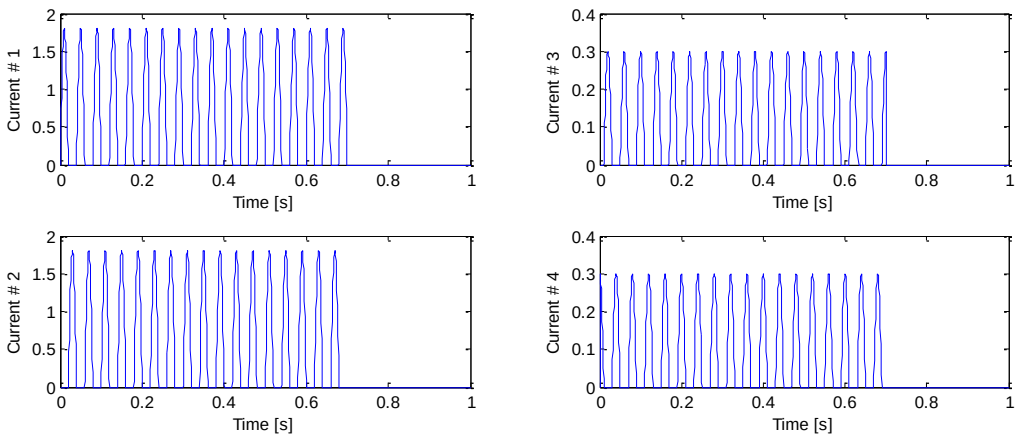

Figure 12. Currents used in the actuator

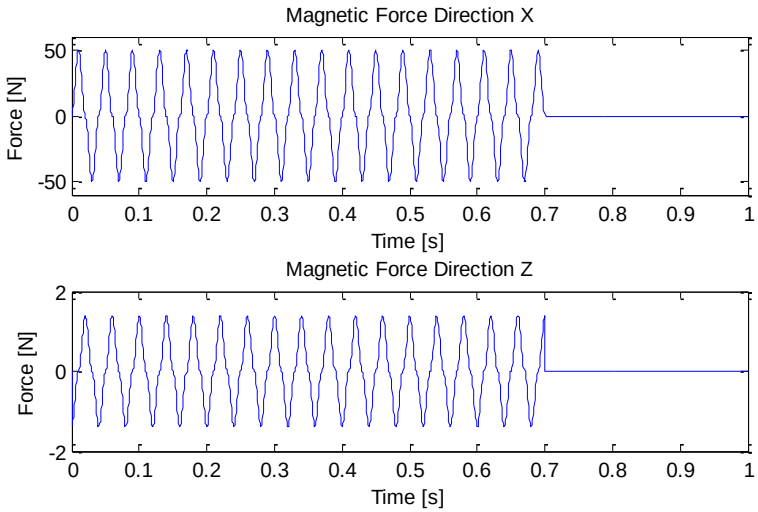

Figure 13. Forces introduced for the breathing mechanism control

5.2. Horizontal Rotor

In this case the crack breathing is given as a function both of the dynamic efforts and of the structure's weight. It is known that the weight itself makes the bending deformation more evident and promotes the crack emergence. The same unbalance and the same rotation speed as for the previous case were considered. The results found by the optimization method for the continuous currents were zero for the coils, except for the coil #3 for which it was found to be 3.105 A. For the varying currents the following amplitude values were obtained: 2.277 A for the coil #1, 2.277 A for the coil #2, 0.435 A for the coil #3, and 0.081 A for the coil #4. Similar to the previous case, the results for the horizontal rotor are presented along 1 second so that the EMA was turned off for t = 0.7 sec. In the Fig. (14) the time responses at the EMA position are shown along the directions x and z, respectively. In the Figs. (15) and (16) we observe the area variation and the second moments of the element cross section. It is possible to observe that the crack is relatively closed. In the Fig. (17) the currents applied to the coils are presented and in the Fig. (18) the corresponding required forces are shown. For the configuration of the currents considered in the present design (see Fig. (7)) the electromagnetic force in the x direction is considerably higher than the one along the z direction.

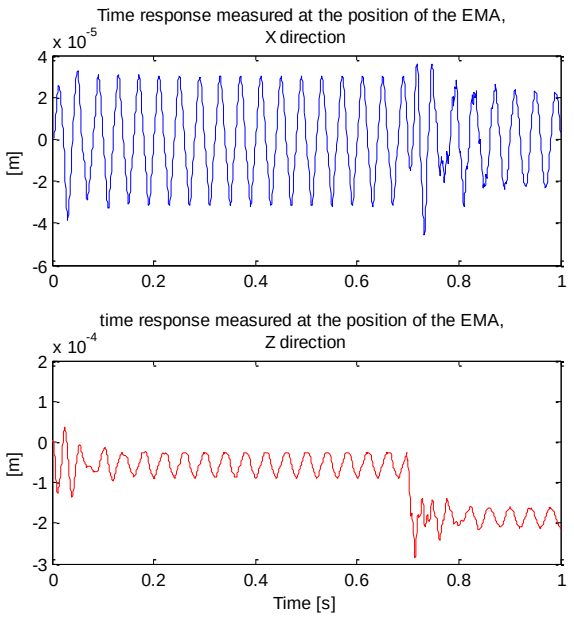

Figure 14. Response of the system

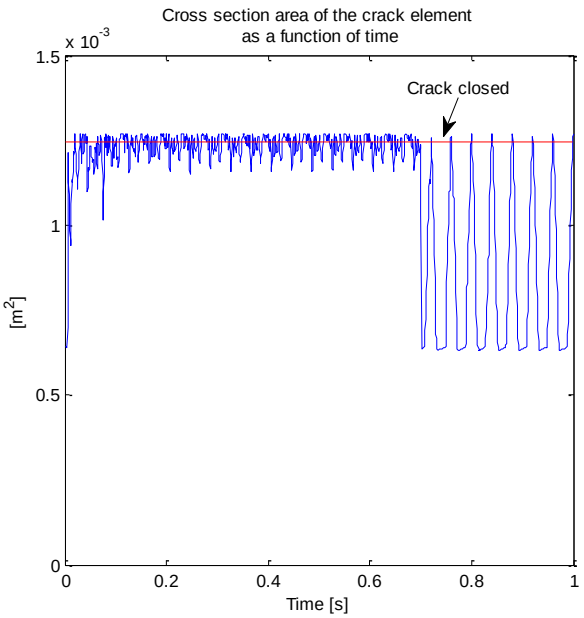

Figure 15. Cross Section of the cracked element

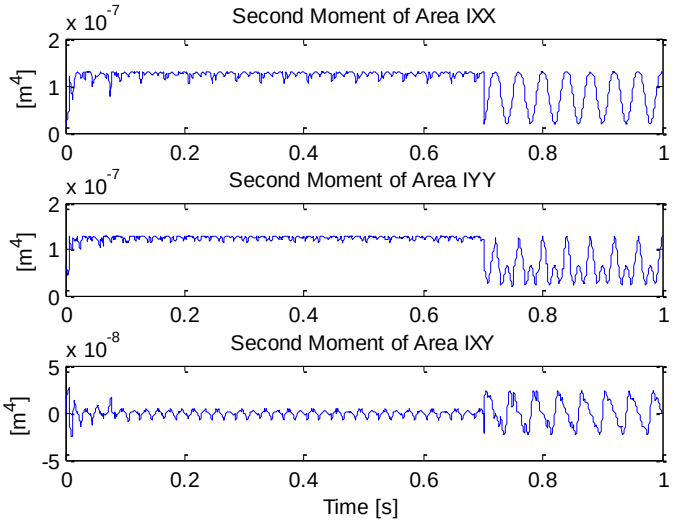

Figure 16. Second Moments of Area

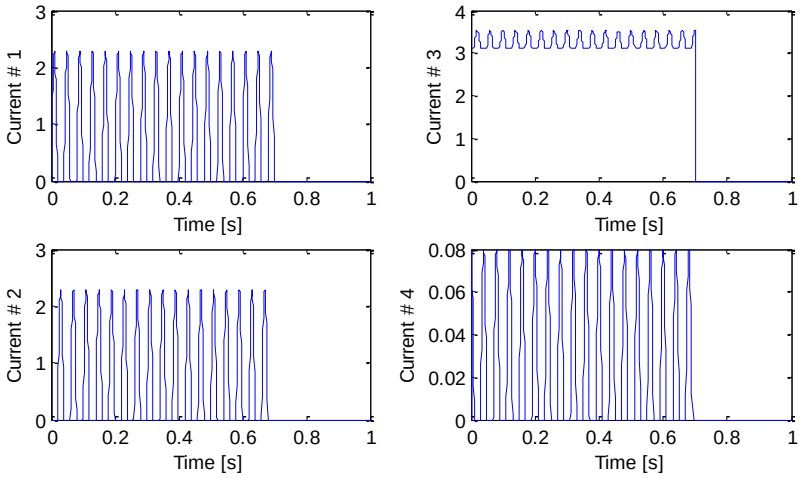

Figure 17. Currents used in the actuator

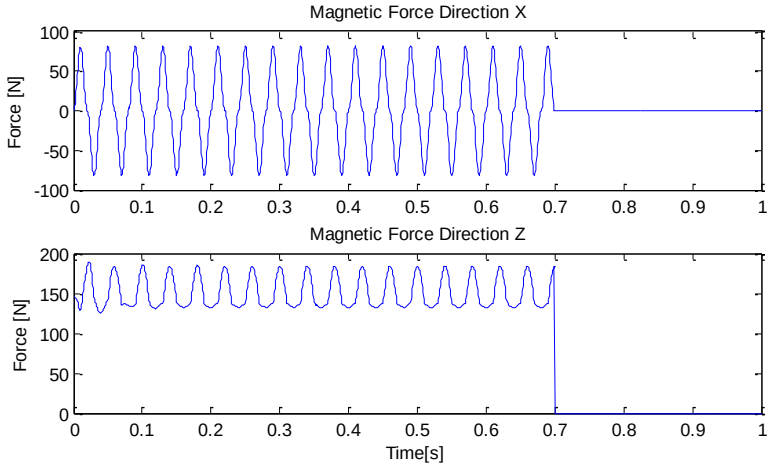

Figure 18. Forces introduced for the breathing mechanism control

6. CONCLUSION

This paper demonstrated the possibility of controlling the fatigue process of a rotating machine by using magnetic actuators. For the identification of the currents to drive the actuators it is required that the following validated models are available: flexible rotor, crack, and electromagnetic actuator. Otherwise, it would be necessary to measure the

resistant cross section area for different time instants, which is virtually impossible. It is expected that the identified currents are able to keep the crack closed when applied to the real system. The crack closure is due to a change in the rotor orbit, as shown in the Fig. (19) where the orbits correspond to the vertical rotor. It was found that the structure does not suffer major changes in the vibration level as depicted in the Figs. (9) and (14); the intensity of the control force plausible from the experimental point of view, as shown in the Figs. (13) and (18). The presented results are given for a specific speed of rotation. Next step would be to observe the behavior of the system for different speed ranges by using high performance controllers such as the neuro fuzzy one.

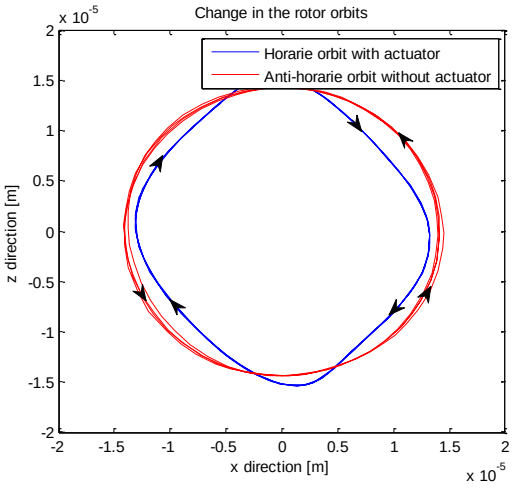

Figure 19. Change in the rotor Orbits

7. ACKNOWLDEGMENTS

The first two authors are thankful to FAPEMIG (TEC 335/2006) and also to FAPEMIG - CNPq (Proc. Nb. 574001/2008-5; INCT-EIE) for providing financial support to this work. The fist author is also thankful to CNPq (Proc. Nb. 200536/2008-7) for the sandwich P.h.d scholarship. The last two authors and the first author wish to thank LaMCoS for material support.

8. REFERENCES

Bachschmid, N., Pennacchi, P., Tanzi, E. and Audebert, S. “Transverse Crack Modeling and Validation in Rotor Systems, Including Thermal Effects” International Journal of Rotating Machinery: 113–126, 2003.

Gasch, R., “A survey of the Dynamic Behaviour of a simple Rotating Shaft with a Transverse Crack” Journal of sound and Vibration, 313-332, 1993.

Mani, G., Quinn, D.D., Kasarda, M. “Active health monitoring in a rotating cracked shaft using active magnetic bearings as force actuators” Journal of Sound and Vibration, 454–465, 2006.

Changsheng, Zhu, Robb, D. A. and Ewins, D. J. “The Dynamic of a Cracked Rotor with an active magnetic bearing” Journal of Sound and Vibration, 469–487, 2003.

Pennacchi, P., Bachschmid, N., and Vania, A., “A model-based identification method of transverse cracks in rotating shafts suitable for industrial machines”, Mechanical Systems and Signal Processing, 2112-2147, 2006.

Lalanne, M. and Ferraris, G. “Rotordynamics Prediction in Engineering”, John Wiley and Sons, Second Edition, 1998.

Damien, G. “Circuit Magnétique – Électroaimant” e-LEE, e-learning for Electrical Engineering, 2003, http://www.lei.ucl.be/multimedia/eLEE/FR/realisations/CircuitsElectriques/index.htm

9. RESPONSIBILITY NOTICE

The author(s) is (are) the only responsible for the printed material included in this paper.